Published in final edited form as:
Dev Dyn. 2012 May ; 241(5): 852–862. doi:10.1002/dvdy.23771.

Inhibitory morphogens and monopodial branching of the embryonic chicken lung

Jason P. Gleghorn[1], **Jiyong Kwak**[1,†], **Amira L. Pavlovich**[1], and **Celeste M. Nelson**[1,2,*]
[1]Department of Chemical and Biological Engineering, Princeton University, Princeton, NJ 08544
[2]Department of Molecular Biology, Princeton University, Princeton, NJ 08544

Abstract

Branching morphogenesis generates a diverse array of epithelial patterns, including dichotomous and monopodial geometries. Dichotomous branching can be instructed by concentration gradients of epithelial-derived inhibitory morphogens, including transforming growth factor-β (TGFβ), which is responsible for ramification of the pubertal mammary gland. Here, we investigated the role of autocrine inhibitory morphogens in monopodial branching morphogenesis of the embryonic chicken lung. Computational modeling and experiments using cultured organ explants each separately revealed that monopodial branching patterns cannot be specified by a single epithelial-derived autocrine morphogen gradient. Instead, signaling via TGFβ1 and bone morphogenetic protein-4 (BMP4) differentially affect the rates of branching and growth of the airways. Allometric analysis revealed that development of the epithelial tree obeys power-law dynamics; TGFβ1 and BMP4 have distinct but reversible effects on the scaling coefficient of the power law. These data suggest that although autocrine inhibition cannot specify monopodial branching, inhibitory morphogens define the dynamics of lung morphogenesis.

Keywords

lateral branching; inhibitory morphogen; patterning; allometry; morphodynamics

Introduction

The tree-like architectures of several organs, including the lung, kidney, and exocrine glands, are sculpted through a process known as branching morphogenesis (Affolter et al., 2003; Lu and Werb, 2008). As with plants, there is enormous diversity in the arborous structures that arise from branching epithelia. The general patterns can be divided into two broad classes: monopodial, in which buds branch laterally off a main stem, and dichotomous, in which the tip of the stem divides to generate two equivalent buds (Davies, 2002). Complex architectures can arise when a single organ develops through a combination of both monopodial and dichotomous branching. How these patterns are generated is an active area of investigation.

Pubertal development of the mouse mammary gland is driven primarily by dichotomous branching, although incipient side branches do form as the result of hormone cycling in adult females of some strains (Gardner and Strong, 1935; Naylor and Ormandy, 2002). This dichotomous pattern of branching is controlled in part by autocrine inhibition through

*Address correspondence to: C.M.N., A321 Engineering Quadrangle, Princeton, NJ 08544, Tel: 609-258-8851, Fax: 609-258-0211, celesten@princeton.edu.
†Current address: Division of Health Sciences and Technology, Massachusetts Institute of Technology, Cambridge, MA 02139

epithelial secretion of transforming growth factor-β (TGFβ) (Gjorevski and Nelson, 2011). All isoforms of TGFβ are expressed by mammary epithelium during its development (Pollard, 2001), and TGFβ1 in particular is concentrated within the periductal sheath (Ewan et al., 2002). Computational models and studies using engineered tissues demonstrated that the concentration gradients of TGFβ that form around the epithelium specify its branching pattern (Nelson et al., 2006; Pavlovich et al., 2011), consistent with branch repulsion seen in the mammary gland *in vivo* (Silberstein and Daniel, 1987; Silberstein et al., 1992). TGFβ is high along the sides of the ducts but low at the ends (Ewan et al., 2002; Nelson et al., 2006), which can bifurcate in response to inductive stimuli. Although members of the TGFβ superfamily are expressed ubiquitously during the morphogenesis of many branched organs (Horowitz and Simons, 2008), the extent to which non-dichotomous branching patterns may be controlled by autocrine inhibition – from these or any other morphogen – is unclear.

Monopodial branching is exemplified by embryonic development of the chicken lung, in which secondary bronchi bud laterally off each primary bronchus. This pattern of branching differs appreciably from that of the more well-studied mammalian lungs, which develop through a combination of monopodial and dichotomous branching (which for the mouse have been designated as domain branching, planar bifurcation, and orthogonal bifurcation) (Metzger et al., 2008; Warburton et al., 2010). Although exogenous addition of TGFβ disrupts branching morphogenesis of mouse lung explants (Serra et al., 1994; Serra and Moses, 1995; Zhao et al., 1998), the major mechanism for patterning the airways is actually through stimulation from signaling centers in the mesenchyme rather than through autocrine inhibition from the epithelium (Morrisey and Hogan, 2010; Warburton et al., 2010). Here, a localized source of fibroblast growth factor-10 (FGF10) in the mesenchyme guides the budding epithelium (Abler et al., 2009). An epithelial source of inhibition does play a role however, as bone morphogenetic protein-4 (BMP4) expressed by the epithelial bud is thought to block the formation of incipient branches in the neighboring epithelium (Bellusci et al., 1996; Weaver et al., 1999; Weaver et al., 2000). As in the mouse (Heine et al., 1990; Pelton et al., 1991; Schmid et al., 1991), BMP4 and other proteins in the TGFβ superfamily are expressed during the development of the embryonic chicken lung (Jakowlew et al., 1992; Jakowlew et al., 1994; Muraoka et al., 2000), suggesting a possible role for inhibitory morphogens in the branching morphogenesis of this organ as well.

Here, we used the embryonic chicken lung as a model system to explore whether and how concentration gradients of TGFβ superfamily members, prototypic inhibitory morphogens, regulate monopodial branching morphogenesis. In particular, we used this system to determine whether autocrine inhibition alone could instruct monopodial branching patterns, as we have seen for dichotomous branching of the mammary gland. We first characterized the branching pattern of lungs *in vivo* and cultured *ex vivo*. We then modeled the three-dimensional (3D) geometry of the airways using computer-aided design (CAD) tools, and calculated the predicted concentration profiles of hypothetical inhibitory morphogens diffusing away from the lung epithelium using the finite element method (FEM). Comparing the branching patterns with the computational results revealed that branching of secondary bronchi is inhibited in regions predicted to be surrounded by high concentrations of inhibitory molecules at the earliest stages of development. At later stages, there was no correlation between sites of secondary bronchi and predicted concentration, suggesting that autocrine inhibition cannot be the major determinant of patterning in this monopodial system. In a separate series of experiments using allometric analysis, we found that monopodial development of the lung obeyed a power-law model which could be described temporally by a master development curve. Manipulating TGFβ1 and BMP4 gradients *ex vivo* revealed that signaling from each differentially inhibited chicken lung development, with TGFβ preferentially blocking branching and BMP4 preferentially blocking growth.

Results

Monopodial branching of the embryonic chicken lung

We examined monopodial branching of the embryonic chicken airways *in vivo* during the window of developmental time in which secondary bronchi bud off of each primary bronchus. E-cadherin staining of whole mounts of embryonic lungs explanted at various Hamburger-Hamilton (HH) stages was used to visualize the development of the epithelial tree (Figure 1). Primary bronchi (mesobronchi) were evident at HH23 and extended in length until branching of secondary bronchi (ventrobronchi) was initiated at HH25. At HH27, the distal end of each primary bronchus dilated to form the vestibulum. Secondary bronchi (both ventrobronchi and dorsobronchi) continued to elongate and branch from and around the main bronchi until HH33, when additional branching from the primary bronchus could not be discerned and other structures such as the air sacs and recurrent bronchi became evident. These observations of the airways visualized using E-cadherin staining are consistent with descriptions gleaned from previously published work using cedar oil or alcian blue histochemistry (Locy and Larsell, 1916a; Locy and Larsell, 1916b; Becchetti et al., 1988).

To control the chemical microenvironment during branching, lungs explanted from HH25- or HH26-stage embryos were cultured at the air-fluid interface on floating membranes *ex vivo*. All cultured explants initially contained one or two secondary bronchi on each primary bronchus. This tight control over the initial morphology of the explants ensured that morphogenesis was limited to monopodial branching from the primary bronchi, and did not include the additional branching or anastomosis of secondary bronchi characteristic of later developmental stages (Figure 1) (Locy and Larsell, 1916a; Locy and Larsell, 1916b; Becchetti et al., 1988). Whereas development of the initial branching pattern of the lung is completed in less than three days *in vivo* (E4+ to E7), lungs cultured *ex vivo* developed more slowly. Cultured explants grew in parallel to the two-dimensional (2D) surface of the membrane, as is common with this technique (Trowell, 1959), with branching sites similar to those observed *in vivo*. After 48 hours, lungs cultured *ex vivo* possessed on average 14 secondary bronchi (7 per primary bronchus), similar to what is observed in HH28-stage embryos.

Computational modeling of autocrine morphogen gradients

The developing lung generates a dynamic chemical environment that, in part, defines its branched structure. At early stages of development, several morphogens are expressed uniformly by the epithelium (Shh, BMP7, canonical Wnts in mouse) (Bellusci et al., 1996; Dean et al., 2005) or found at uniformly high concentrations just basal to the epithelium (TGFβ1, TGFβ2, TGFβ3) (Heine et al., 1990; Pelton et al., 1991). As tissue geometry can sculpt the concentration profiles of morphogens (Nelson, 2009), we used computational models to explore whether signaling from autocrine morphogen gradients could play a decisive role in defining the monopodial pattern of the embryonic airways.

The E-cadherin immunofluorescence staining described above was used to create 3D solid models of the lung epithelial tree at various stages of development (Figure 2). These solid models contained between zero (HH24) and eight (HH27+) secondary bronchi that matched the angles and dimensions of the airways within the whole lung explants. The solid model renderings were then used to calculate numerically the steady-state concentration profile of an arbitrary hypothetical morphogen secreted by and diffusing away from the airway epithelium.

As expected, the concentration profile predicted numerically changed as the geometry of the airways changed. At HH24, prior to budding of the secondary bronchi, the predicted

morphogen concentration is maximal where the trachea bifurcates and the two primary bronchi are in close proximity to each other (Figure 2A). The morphogen concentration then decreases laterally from the sides as well as distally toward the tips of the primary bronchi into the mesenchyme. This general concentration profile is maintained through HH27 (Figure 2B–E). However, as secondary bronchi form in the models of lungs at stages HH25 and later, local changes in concentration arise relative to the branches. For all models that contained secondary bronchi, a local maximum in concentration is predicted at the site where the bud branches off the primary bronchus (Figure 2F–H). The concentration profile then decreases along the length of each secondary bronchus, resulting in a local minimum in morphogen concentration at the distal tip of the bud.

Whereas it is clear that these computational studies predict a dynamic chemical environment with local gradients on the scale of morphological features, these models suggest that a morphogen secreted by and diffusing away from the epithelium cannot be the major mechanism used to define the monopodial branching pattern of the embryonic chicken lung. The sites of branching in lung explants do not correlate with local maxima or minima in the predicted concentration of morphogen. Nonetheless, regions of local maxima, proximally along the primary bronchi and at clefts around branch points, do correlate with areas of TGFβ1 localization reported in the mouse lung (Heine et al., 1990; Pelton et al., 1991). These results suggest that though high concentrations of inhibitory morphogens may suppress branching, other factors are likely involved in determining the sites at which the secondary bronchi branch off of the primary airways. Monopodial branching of the embryonic chicken airways is thus distinct from dichotomous branching of the murine mammary gland.

Disruption of TGFβ signaling

Since it was clear from our computational models that autocrine inhibitory morphogens alone do not specify branch sites, we set out to quantify the relative roles played by the major inhibitors in development of the chicken airways. TGFβ is a prototypic inhibitory morphogen that is expressed uniformly within the embryonic chicken lung during the stages of monopodial branching off of the primary bronchi (Figure S1). To quantify the relative role of TGFβ signaling in the regulation of monopodial branching morphogenesis of the chicken lung, we used two approaches to disrupt its endogenous concentration profile in cultured explants. In the first approach we added recombinant TGFβ1 to the explant, thereby exposing the tissue to a uniformly high concentration of morphogen. Treatment with recombinant TGFβ1 inhibited branching in a dose-dependent manner (Figure 3A, B), with a striking reduction in both the number of buds and the size of the organ following 24 and 48 hours of culture. Minimal branching was observed in explants treated with TGFβ1, which only initiated one or two buds over 48 hours as compared to controls, which initiated ~14 buds. Addition of TGFβ1 also inhibited elongation and growth of both primary and secondary bronchi, as assessed by measuring the fold change in the projected area of the lumen of the airways (Figure 3C). Our second approach to disrupt the endogenous TGFβ concentration profile was to treat explants with a pharmacological inhibitor of the Alk5 type I TGFβ receptor (TβRI) kinase, thereby blocking signaling of all TGFβ isoforms. Inhibiting TβRI enhanced branching of the lung explants, which initiated ~16–17 buds over 48 hours of culture (Figure 3A, B). Blocking the receptor also led to a decrease in the overall size of the lungs, as compared to controls (Figure 3C).

Although both recombinant TGFβ1 and the TβRI inhibitor altered the number and size of secondary bronchi, neither affected the sites at which these budded off of the primary bronchus. We arrived at this conclusion using morphometric analysis, wherein we quantified the length of the primary bronchus (*L*) and the relative position of each secondary bronchus (*b1, b2, b3, b4*) as a function of this length (Figure 4A). Analysis of control explants

revealed that, at 48 hours of culture, the first secondary bronchus (*b1*) emerged at a position ~52% down the length of the primary bronchus, as measured from the point of the tracheal bifurcation ($T\text{-}b1 = 0.52 \cdot L$). This distance was highly reproducible between explants. The distance between the first and second ventrobronchi was ~5% of the length of the primary bronchus ($b1\text{–}b2 = 0.05 \cdot L$). Subsequent secondary bronchi (*b3, b4*) also formed at predictable and reproducible positions along the primary bronchus. Manipulating TGFβ signaling using either recombinant growth factor or TβRI inhibitor decreased the length of the primary bronchus (L), but did not affect the relative position of the secondary bronchi: *b1* always formed at a position ~52% down the length of the primary bronchus, and later buds were similarly unaltered in their relative location. These data suggest that branch sites are determined relative to the scaling of the entire organ, rather than set at fixed positions.

Secondary bronchi formed at consistent and predictable locations, even though the size of the organ decreased dramatically with TGFβ manipulation, as reflected in the morphometric parameter L. There were two possible explanations for the constant positioning: either there were fewer cells in between secondary bronchi or the cells were smaller in size. To distinguish between these possibilities, we counted the number of epithelial cells as a function of distance along the primary bronchus (Figure 4B). For control explants, we found ~18 cells between the *b1* and *b2* secondary bronchi; as with the morphometric analysis, this number was highly reproducible between samples. We found ~15 cells between *b2* and *b3*, and ~23 cells between *b3* and *b4*. Manipulating TGFβ signaling caused a marked decrease in the number of cells in the primary bronchus between emerging branches, and a corresponding decrease in cell proliferation (Figure S2). These data are consistent with the conclusion that branch sites are determined relative to the scaling of the organ, and suggest that TGFβ signaling affects the rate at which these branches emerge rather then their location along the primary bronchus.

Disruption of BMP signaling

BMP4 is a member of the TGFβ superfamily that plays a major role in the morphogenesis of mammalian airways. In the embryonic mouse lung, inhibitory signaling from BMP4 restricts incipient branching adjacent to nascent buds (Lebeche et al., 1999; Weaver et al., 1999; Weaver et al., 2000). BMP4 is expressed within the epithelium of the primary bronchus in the chicken airways, and at higher levels in newly forming secondary bronchi (Figure S1). To determine the role of BMP4 in monopodial branching of the chicken lung, we disrupted its endogenous concentration profile in cultured explants. Addition of recombinant BMP4 had no effect on the budding of secondary bronchi; BMP4-treated explants formed ~14 buds over 48 hours of culture, indistinguishable from controls (Figure 5A, B). However, treatment with BMP4 did decrease the overall growth of the organ explants in a dose-dependent manner (Figure 5C). Conversely, treatment with dorsomorphin, which inhibits the kinase activity of the Alk3 and Alk6 type I BMP receptors (BMPRI) (Yu et al., 2008), significantly reduced the number of buds that formed (Figure 5A, B). Curiously, inhibiting BMPRI caused an increase in overall growth of the lungs and swelling of the airway lumena (Figure 5C) and proliferation of the epithelium (Figure S2). As with TGFβ1, manipulating BMP4 signaling had no effect on the relative sites along the primary bronchus at which secondary bronchi formed (Figure 4A, B). These data suggested that neither TGFβ1 nor BMP4 specified sites of monopodial branching. Consistent with this interpretation, we found that pSmad2/3 and pSmad1/5/8 were present in the nuclei of cells along the primary bronchus and in nascent secondary bronchi (Figure S1), again suggesting that branch sites are not determined by signaling downstream of TGFβ or BMP.

Allometric analysis of lung growth

The data described above revealed that TGFβ1 and BMP4 may play different roles in monopodial branching of the chicken lung. To compare the branching patterns between treatment groups quantitatively, we created an analysis framework based on the principles of allometry to relate the extent of branching and the size of the branched structure. Allometry is the study of the relationship between body size and geometrical, anatomical, physiological, or behavioral variables and effectively describes the scaling behavior of the variables (Shingleton et al., 2007). In biological systems, a power-law model of the form $y \propto x^a$ is commonly used to describe the relationship between the two measured variables (Huxley, 1924; Huxley and Tessier, 1936).

For the purposes of this study, we were interested in how the epithelial tree changes during monopodial branching and how inhibitory morphogens modulate that structure. To that end, we analyzed the fold change in the extent of branching (allometric growth) relative to the fold change in the lumen area (isometric growth) (Figure 6A). Surprisingly, data points from individual control explants that were tracked over time collapsed onto a single master "development curve" that was well described by a power-law model (scaling coefficient: a=1.69, R^2=0.95). That the scaling ratio between isometric and allometric growth is well described by a single master curve demonstrates that monopodial growth of the epithelial tree is stereotyped – consistent and predictable – in this *ex vivo* system. Additionally, the temporal nature of this analysis framework enabled the creation of a "state diagram" that defines the structure and size of the epithelial tree at any given time (Figure 6B). The state diagram permitted us to easily identify and characterize the changes in the morphology of the epithelial tree resulting from different treatments. Explants treated exogenously with recombinant TGFβ1 fell on top of the development curve; however, development of the epithelial tree was significantly delayed and essentially arrested in time (Figure 6C). Treatment with the TβRI inhibitor resulted in explants that fell in the upper left quadrant of the state diagram, smaller lungs with hyperplastic branching. Explants treated with recombinant BMP4 branched to the same extent as controls, but the size of the epithelial tree decreased with increasing concentration (Figure 6D). Conversely, treatment with the BMPRI inhibitor produced large hypoplastic lungs, which fell in the lower right quadrant of the state diagram.

The allometric analysis thus suggested that signaling through TβRI and BMPRI differentially affected branching and growth. This hypothesis was supported by the results from washout experiments, in which we treated explants with recombinant growth factor or receptor inhibitor for 24 hours, and then removed treatment and followed the morphology after an additional 24 hours (Figure 6E,F). Allometric analysis confirmed that high concentrations of TGFβ1, delivered exogenously, arrested development of the lung, as both 24-hour and 48-hour treatments exhibited the same morphology on the master development curve (Figure 6E). Washing out TGFβ1 released the arrest and allowed the lungs to recover to near control morphology. Inhibiting TβRI consistently led to small lungs with hyperplastic branching as compared to controls at each time point. Washing out the TβRI inhibitor permitted the lungs to develop to a near normal morphology, suggesting that the effects of the inhibitor are reversible. These data suggest that signaling through TβRI inhibits branching in favor of growth.

Allometric analysis revealed the opposite effect for BMP signaling. High concentrations of recombinant BMP4 inhibited growth without affecting branching, producing small lungs with the same number of buds as controls at both time points (Figure 6F). Washing out BMP4 shifted the lungs back to the master development curve, permitting the size of the lungs to recover from the treatment. Inhibiting BMPRI led to hypoplastic branching, with enhanced growth after longer time points. Washing out the inhibitor again shifted the lungs

back to the master development curve, although these samples appeared to have a significant developmental delay. These data suggest that signaling through BMPRI inhibits growth in favor of branching. Inhibitory morphogens of the TGFβ superfamily thus play distinct roles in the monopodial morphogenesis of the embryonic chicken lung.

Discussion

The development of the branching patterns of epithelial trees has fascinated scientists for several generations (Metzger and Krasnow, 1999). Many of the molecular and physical rules that govern branching morphogenesis have been uncovered for specific model organs (Costantini and Kopan, 2010; Larsen et al., 2010; Warburton et al., 2010; McNally and Martin, 2011). In dichotomous branching of the mouse mammary epithelial tree, the epithelium defines its own sites of branching by secreting the inhibitory morphogen, TGFβ1 (Gjorevski and Nelson, 2011). Here, computational modeling and cultured organ explants separately revealed that autocrine inhibition is not the primary mechanism that controls the pattern of monopodial branching of the embryonic chicken lung. In fact, our computational model suggests that no single morphogen secreted uniformly from the epithelium can define monopodial branching patterns. Autocrine inhibition and branch repulsion may thus be unique to ramification via dichotomous branching.

Although they did not specify the relative *sites* of monopodial branching, two prototypic inhibitory morphogens, TGFβ1 and BMP4, did differentially affect development of embryonic chicken airways in explant cultures (Figure 7). Indeed, we found that signaling through TGFβ receptors blocked branching, but enhanced growth. Conversely, signaling through BMP receptors enhanced branching but blocked growth. Consistent with these conclusions, we found that inhibiting TβRI led to decreased proliferation of the airway epithelial cells, whereas inhibiting BMPRI led to enhanced proliferation of the airway epithelium as compared to controls (Figure S2). Morphometric analysis revealed that neither TGFβ1 nor BMP4 altered the relative sites of branching, but instead affected the *rate* at which new branches formed along the primary bronchus. These data suggest that branching and growth of the epithelial tree may be coupled and inversely correlated, at least during these stages of monopodial morphogenesis. The signaling switches that discern branching from growth, as well as the cellular behaviors responsible for the gross alterations in morphology, remain to be elucidated. Nonetheless, recent studies of the mouse lung found that division axis is tightly regulated during the morphogenesis of that organ (Tang et al., 2011), suggesting the tantalizing possibility that TGFβ and BMP may conspire to determine spindle orientation.

It is important to note that the effects of TGFβ1 and BMP4 uncovered here are not entirely consistent with the roles of these morphogens in the embryonic development of the mouse lung. TGFβ signaling inhibits branching of both mouse and chicken airways (Serra et al., 1994; Serra and Moses, 1995; Zhao et al., 1996; Zhao et al., 1998; Zhao et al., 2000; Stabellini et al., 2001), but disrupting signaling through the receptor only appears to block growth of the airways in explant cultures of the chicken lung. In contrast, blocking TGFβ receptor signaling in culture or *in vivo* enhances branching of the mouse lung without reportedly affecting growth of the airways (Zhao et al., 1996; Zhao et al., 1998). BMP4 signaling inhibits FGF10-induced branching of the mouse airway epithelium (Bellusci et al., 1996; Weaver et al., 1999; Weaver et al., 2000), but instead primarily inhibits growth of the chicken airways. In the mouse, BMP4 is known to block cell proliferation, as treatment with exogenous BMP4 reduces incorporation of BrdU (Weaver et al., 2000) and transgenic overexpression of BMP4 in the distal epithelium results in smaller lungs with decreased proliferation (Bellusci et al., 1996). It is unclear why BMP4 did not also inhibit branching in the chicken lung explant cultures described here. Analysis of BMP4-treated explants

revealed subtle effects on proliferation, with an overall decrease in epithelial incorporation of the BrdU analog, EdU (Figure S2). However, BMP4 has been reported to stimulate the branching of mouse lung bud cultures when both epithelium and mesenchyme are present (Bragg et al., 2001; Shi et al., 2001), suggesting that experimental context may be particularly critical in the signaling of this molecule. Further work is needed to define the differences between TGFβ and BMP signaling in simple monopodial branching (as seen in the chicken) and combination monopodial/dichotomous branching (as seen in the mouse).

Even though manipulating TGFβ and BMP receptor signaling had large effects on the gross morphology of the lungs, neither affected the relative positioning of the buds along the primary bronchi. Surprisingly, each secondary bronchus always formed at a precise fractional position relative to the length of the primary bronchus, irrespective of treatment condition. These data are consistent with the notion that TGFβ and BMP4 affect the rate at which new branches form relative to control lungs, but do not affect sites of branching. These data also suggest that monopodial branching patterns scale with overall lung size in the chicken, and that branch sites are determined by signals regulated by this scaling. Such a scaling is reminiscent of patterning in the early *Drosophila* embryo, wherein the shape of the Bicoid concentration gradient and position of the segmentation genes scale across species with five-fold differences in size (Gregor et al., 2005); how this occurs is still a mystery. In the mouse, sites of branching are thought to be specified by localized sources of FGF10 in the mesenchyme (Abler et al., 2009). A recent study showed that FGF10 is also expressed in the mesenchyme in the embryonic chicken lung and is required for epithelial branching (Moura et al., 2011). Whether this signaling scales with overall lung size to determine branch sites along the primary bronchus remains to be determined.

Finally, careful morphometric analysis of the lungs at different stages and with different treatments permitted us to create an allometric analysis framework that could describe monopodial morphogenesis of the airways with a single mathematical equation in the form of a power law. Power laws are closely related to fractal behavior and have been used extensively to describe different aspects of the anatomy and physiology of the adult lung (Suki et al., 1994; Suki, 2002). As applied to the embryonic organ, our power-law model of monopodial morphogenesis enabled objective, quantitative comparisons across developmental time and experimental manipulations. We found that for explants, branching was proportional to the projected area of the airways raised to ~3/2 power. This scaling exponent is consistent with qualitative observations that the lungs branch faster than they grow in size, a necessary condition for a space-filling ramified architecture. Allometric analysis of embryonic development may prove useful for a wide variety of organs and organ systems, and will likely enable objective and quantitative comparisons to be made between observations published independently by different investigators.

Experimental Procedures

Immunofluorescence staining

Fertilized chicken (*Gallus gallus* variant *domesticus*, White Leghorn) eggs were obtained from a commercial vendor and incubated at 38°C in a humidified atmosphere to allow for embryonic development. Whole embryonic lungs were microdissected over a range of Hamburger-Hamilton (HH) stages (Hamburger and Hamilton, 1951) and fixed in 4% paraformaldehyde in phosphate-buffered saline (PBS) for 15 minutes at room temperature.

For whole mount staining of E-cadherin, fixed samples were washed twice with PBS and serially dehydrated in increasing concentrations of methanol/PBS. Samples were incubated in 5% H_2O_2/methanol for 5 hours and serially rehydrated in decreasing concentrations of methanol in 0.1% Tween-20/PBS. Samples were blocked with 10% goat serum/PBS/0.5%

Triton X-100 (GPT) and subsequently incubated overnight at 4°C with 1:50 mouse anti-E-cadherin (LCAM) (Developmental Studies Hybridoma Bank) in 5% GPT. Samples were washed in 5% GPT and incubated overnight with 1:500 biotinylated goat anti-mouse IgG (Vector Laboratories) in 5% GPT at 4°C. The following day, samples were incubated with ABC Elite Reagent (Vector Laboratories) for 2 hours, washed in 5% GPT, and then incubated in 1:100 SA-HRP Fluorescein Tyramide Reagent (Perkin Elmer) for 30 minutes. Samples were then washed in 0.1M Tris-Cl/1.5M NaCl/Tween 20 (TNT) and mounted in Vectashield (Vector Laboratories) for imaging.

For staining of sections, samples were embedded in low-melt agarose (Sigma) and sectioned into 100-μm -thick sections on a vibratome (Ted Pella). Sections were blocked with 10% GPT and incubated at 4°C overnight with primary antibody [1:100 pSmad 2/3 (Santa Cruz Biotechnology) or 1:100 pSmad 1/5/8 (Cell Signaling)] in 5% GPT. The following day, samples were washed with 5% GPT and incubated in 1:500 biotinylated goat anti-mouse IgG for 3 hours. Lung sections were subsequently washed with 5% GPT, incubated with ABC Elite reagent for 30 minutes, washed again with 5% GPT, and then incubated in 1:100 SA-HRP Fluorescein Tyramide Reagent for 15 minutes. Finally, samples were washed with TNT buffer and mounted for imaging.

For staining of TGFβ and BMP4, whole explants were blocked in GPT and incubated overnight at 4°C with 1:100 anti-TGFβ1 (Cell Signaling) or anti-BMP4 (BioVision) in 5% GPT. Samples were washed in 5% GPT and incubated overnight with 1:100 Alexa-tagged secondary antibodies (Invitrogen) in 5% GPT at 4°C. The following day, samples were washed extensively and mounted for imaging.

For analysis of proliferation, EdU incorporation was performed using the Click-iT EdU Alexa Fluor 594 Imaging Kit (Invitrogen) according to the manufacturer's protocol.

Computational modeling of morphogen gradients

Fluorescent images of E-cadherin staining in whole mounts were analyzed with ImageJ (National Institutes of Health) to determine morphometric parameters that define the diameters and lengths of the primary and secondary bronchi, as well as the position of the secondary bronchi along the length of the primary bronchus. Three-dimensional (3D) computer-aided design (CAD) solid models of the epithelial airways were created with Autodesk Inventor 2010 (Autodesk) for lungs at different stages of development.

The 3D concentration profile of autocrine-secreted morphogen diffusing away from the lung epithelium was calculated using COMSOL Multiphysics (COMSOL Inc.). CAD models of the lung epithelium were confined to a cylindrical bounding box, 40-mm in diameter and 40-mm tall. This bounding box represents an essentially infinite volume (~ 320,000-fold the volume of the lumen) with the properties of water. Constant uniform secretion of the morphogen from the lung epithelium was enforced with the flux from the surface of the epithelium set to 1, and passive isotropic diffusion through the mesenchyme was assumed. Partial differential equations that define the concentration profiles

$$D\nabla^2 C=0$$

were solved using the finite element method (FEM), with boundary conditions of constant flux at the epithelial surface:

$$D\frac{\partial C}{\partial x}\Big|_{x=x_0} = D\frac{\partial C}{\partial y}\Big|_{y=y_0} = D\frac{\partial C}{\partial z}\Big|_{z=z_0} = 1$$

and zero sink far from the epithelium:

$$x, y, z \to \infty,\ C \to 0.$$

where C is the concentration of hypothetical inhibitor and D is the diffusion coefficient for the hypothetical inhibitor within the surrounding mesenchyme. We assume that D is constant throughout the volume of the mesenchyme, but note that large variations in the composition of the extracellular matrix or packing of mesenchymal cells may impact the effective relative diffusivity (Miura et al., 2009). The steady-state 3D concentration profiles were normalized to the maximum concentration of the most developed lung epithelial tree, enabling comparison of predicted concentration profiles over the course of lung development.

Ex vivo culture of embryonic lungs

Whole embryonic lungs were microdissected at stages HH25-26 (2–4 buds) in PBS supplemented with 100 U/mL penicillin and 100 μg/mL streptomycin (Invitrogen). After dissection, lungs were cultured at the air-fluid interface on a floating raft (Trowell, 1959). Two or three embryonic lungs were placed on a membrane (11-μm pore diameter; Whatman) floating on BGJb medium (Invitrogen) supplemented with 100 U/mL penicillin, 100 μg/mL streptomycin (Invitrogen) and 0.2 mg/mL ascorbic acid (Sigma).

Experimental conditions included the addition of recombinant human TGFβ1 (R&D Systems), recombinant human BMP4 (R&D Systems), Alk5 inhibitor I (Calbiochem), or dorsomorphin (Tocris Bioscience) to the complete media formulation. Lungs were cultured over 48 hours under optimal humidity at 37°C in 5% CO_2, with media changed after 24 hours. For washout experiments, lungs were cultured in the presence of growth factor or inhibitor as above for 24 hours. The media was then replaced with fresh complete media, and lungs were incubated for an additional 24 hours.

Allometric analysis

Brightfield images of the cultured lungs were taken with a stereomicroscope (Nikon) and buds were enumerated at 0, 24, and 48 hours. As a measure of the relative size of the epithelial trees between treatment groups, images were thresholded and a two-dimensional (2D) projection of the area of the lumen was analyzed using ImageJ.

Supplementary Material

Refer to Web version on PubMed Central for supplementary material.

Acknowledgments

Grant Sponsors: David & Lucile Packard Foundation; Alfred P. Sloan Foundation; NIH, grant numbers: GM083997 and HL110335.

We thank Maya Anjur-Dietrich and Alyssa Mancini for technical assistance. C.M.N. holds a Career Award at the Scientific Interface from the Burroughs Wellcome Fund. J.K. was supported by a Samsung Scholarship and the Rudlin senior thesis fund.

Abbreviations

αSMA	alpha-smooth muscle actin
ALK	activin-like kinase
BMP	bone morphogenetic protein
BMPRI	BMP receptor type I
CAD	computer-aided design
E	embryonic day
FEM	finite element method
FGF	fibroblast growth factor
HH	Hamburger-Hamilton
LCAM	liver cell adhesion molecule
TGFβ	transforming growth factor-beta
TβRI	TGFβ receptor type I
2D	two-dimension(al)
3D	three-dimension(al)

References

Abler LL, Mansour SL, Sun X. Conditional gene inactivation reveals roles for Fgf10 and Fgfr2 in establishing a normal pattern of epithelial branching in the mouse lung. Dev Dyn. 2009; 238:1999–2013. [PubMed: 19618463]

Affolter M, Bellusci S, Itoh N, Shilo B, Thiery JP, Werb Z. Tube or not tube: remodeling epithelial tissues by branching morphogenesis. Dev Cell. 2003; 4:11–18. [PubMed: 12530959]

Becchetti E, Evangelisti R, Stabellini G, Pagliarini A, del Borrello E, Calastrini C, Carinci P. Developmental heterogeneity of mesenchymal glycosaminoglycans (GAG) distribution in chick embryo lung anlagen. Am J Anat. 1988; 181:33–42. [PubMed: 3348146]

Bellusci S, Henderson R, Winnier G, Oikawa T, Hogan BL. Evidence from normal expression and targeted misexpression that bone morphogenetic protein (Bmp-4) plays a role in mouse embryonic lung morphogenesis. Development. 1996; 122:1693–1702. [PubMed: 8674409]

Bragg AD, Moses HL, Serra R. Signaling to the epithelium is not sufficient to mediate all of the effects of transforming growth factor beta and bone morphogenetic protein 4 on murine embryonic lung development. Mech Dev. 2001; 109:13–26. [PubMed: 11677049]

Costantini F, Kopan R. Patterning a complex organ: Branching morphogenesis and nephron segmentation in kidney development. Dev Cell. 2010; 18:698–712. [PubMed: 20493806]

Davies JA. Do different branching epithelia use a conserved developmental mechanism? BioEssays. 2002; 24:937–948. [PubMed: 12325126]

Dean CH, Miller LA, Smith AN, Dufort D, Lang RA, Niswander LA. Canonical Wnt signaling negatively regulates branching morphogenesis of the lung and lacrimal gland. Dev Biol. 2005; 286:270–286. [PubMed: 16126193]

Ewan KB, Shyamala G, Ravani SA, Tang Y, Akhurst R, Wakefield L, Barcellos-Hoff MH. Latent transforming growth factor-beta activation in mammary gland: regulation by ovarian hormones affects ductal and alveolar proliferation. Am J Pathol. 2002; 160:2081–2093. [PubMed: 12057913]

Gardner WU, Strong LC. The normal development of the mammary glands of virgin female mice of ten strains vary in susceptibility to spontaneous neoplasms. Am J Cancer. 1935; 25:282–290.

Gjorevski N, Nelson CM. Integrated morphodynamic signalling of the mammary gland. Nat Rev Mol Cell Biol. 2011; 12:581–593. [PubMed: 21829222]

Gregor T, Bialek W, de Ruyter van Steveninck RR, Tank DW, Wieschaus EF. Diffusion and scaling during early embryonic pattern formation. Proc Natl Acad Sci U S A. 2005; 102:18403–18407. [PubMed: 16352710]

Hamburger V, Hamilton HL. A series of normal stages in the development of the chick embryo. J Morphol. 1951; 88:49–92.

Heine UI, Munoz EF, Flanders KC, Roberts AB, Sporn MB. Colocalization of TGF-beta 1 and collagen I and III, fibronectin and glycosaminoglycans during lung branching morphogenesis. Development. 1990; 109:29–36. [PubMed: 2209468]

Horowitz A, Simons M. Branching morphogenesis. Circ Res. 2008; 103:784–795. [PubMed: 18845818]

Huxley J. Constant differential growth-ratios and their significance. Nature. 1924; 114:895–896.

Huxley J, Tessier G. Terminology of relative growth. Nature. 1936; 137:780–781.

Jakowlew SB, Ciment G, Tuan RS, Sporn MB, Roberts AB. Pattern of expression of transforming growth factor-beta 4 mRNA and protein in the developing chicken embryo. Dev Dyn. 1992; 195:276–289. [PubMed: 1304823]

Jakowlew SB, Ciment G, Tuan RS, Sporn MB, Roberts AB. Expression of transforming growth factor-beta 2 and beta 3 mRNAs and proteins in the developing chicken embryo. Differentiation. 1994; 55:105–118. [PubMed: 8143928]

Larsen M, Yamada KM, Musselmann K. Systems analysis of salivary gland development and disease. Wiley Interdiscip Rev Systems Biol Med. 2010

Lebeche D, Malpel S, Cardoso WV. Fibroblast growth factor interactions in the developing lung. Mech Dev. 1999; 86:125–136. [PubMed: 10446271]

Locy WA, Larsell O. The embryology of the bird's lung based on observations of the domestic fowl, part I. Am J Anat. 1916a; 19:447–504.

Locy WA, Larsell O. The embryology of the bird's lung based on observations of the domestic fowl, part II. Am J Anat. 1916b; 20:1–44.

Lu P, Werb Z. Patterning mechanisms of branched organs. Science. 2008; 322:1506–1509. [PubMed: 19056977]

McNally S, Martin F. Molecular regulators of pubertal mammary gland development. Ann Med. 2011; 43:212–234. [PubMed: 21417804]

Metzger RJ, Klein OD, Martin GR, Krasnow MA. The branching programme of mouse lung development. Nature. 2008; 453:745–750. [PubMed: 18463632]

Metzger RJ, Krasnow MA. Genetic control of branching morphogenesis. Science. 1999; 284:1635–1639. [PubMed: 10383344]

Miura T, Hartmann D, Kinboshi M, Komada M, Ishibashi M, Shiota K. The cyst-branch difference in developing chick lung results from a different morphogen diffusion coefficient. Mech Dev. 2009; 126:160–172. [PubMed: 19073251]

Morrisey EE, Hogan BL. Preparing for the First Breath: Genetic and Cellular Mechanisms in Lung Development. Dev Cell. 2010; 18:8–23. [PubMed: 20152174]

Moura RS, Coutinho-Borges JP, Pacheco AP, Damota PO, Correia-Pinto J. FGF signaling pathway in the developing chick lung: expression and inhibition studies. PLoS One. 2011; 6:e17660. [PubMed: 21412430]

Muraoka RS, Bushdid PB, Brantley DM, Yull FE, Kerr LD. Mesenchymal expression of nuclear factor-kappaB inhibits epithelial growth and branching in the embryonic chick lung. Dev Biol. 2000; 225:322–338. [PubMed: 10985853]

Naylor MJ, Ormandy CJ. Mouse strain-specific patterns of mammary epithelial ductal side branching are elicited by stromal factors. Dev Dyn. 2002; 225:100–105. [PubMed: 12203726]

Nelson CM. Geometric control of tissue morphogenesis. Biochim Biophys Acta. 2009; 1793:903–910. [PubMed: 19167433]

Nelson CM, Vanduijn MM, Inman JL, Fletcher DA, Bissell MJ. Tissue geometry determines sites of mammary branching morphogenesis in organotypic cultures. Science. 2006; 314:298–300. [PubMed: 17038622]

Pavlovich AL, Boghaert E, Nelson CM. Mammary branch initiation and extension are inhibited by separate pathways downstream of TGFbeta in culture. Exp Cell Res. 2011; 317:1872–1884. [PubMed: 21459084]

Pelton RW, Saxena B, Jones M, Moses HL, Gold LI. Immunohistochemical localization of TGF beta 1, TGF beta 2, and TGF beta 3 in the mouse embryo: expression patterns suggest multiple roles during embryonic development. J Cell Biol. 1991; 115:1091–1105. [PubMed: 1955457]

Pollard JW. Tumour-stromal interactions. Transforming growth factor-beta isoforms and hepatocyte growth factor/scatter factor in mammary gland ductal morphogenesis. Breast Cancer Res. 2001; 3:230–237. [PubMed: 11434874]

Schmid P, Cox D, Bilbe G, Maier R, McMaster GK. Differential expression of TGF beta 1, beta 2 and beta 3 genes during mouse embryogenesis. Development. 1991; 111:117–130. [PubMed: 2015789]

Serra R, Moses HL. pRb is necessary for inhibition of N-myc expression by TGF-beta 1 in embryonic lung organ cultures. Development. 1995; 121:3057–3066. [PubMed: 7555731]

Serra R, Pelton RW, Moses HL. TGF beta 1 inhibits branching morphogenesis and N-myc expression in lung bud organ cultures. Development. 1994; 120:2153–2161. [PubMed: 7523056]

Shi W, Zhao J, Anderson KD, Warburton D. Gremlin negatively modulates BMP-4 induction of embryonic mouse lung branching morphogenesis. Am J Physiol Lung Cell Mol Physiol. 2001; 280:L1030–1039. [PubMed: 11290528]

Shingleton AW, Frankino WA, Flatt T, Nijhout HF, Emlen DJ. Size and shape: the developmental regulation of static allometry in insects. BioEssays. 2007; 29:536–548. [PubMed: 17508394]

Silberstein GB, Daniel CW. Reversible inhibition of mammary gland growth by transforming growth factor-beta. Science. 1987; 237:291–293. [PubMed: 3474783]

Silberstein GB, Flanders KC, Roberts AB, Daniel CW. Regulation of mammary morphogenesis: evidence for extracellular matrix-mediated inhibition of ductal budding by transforming growth factor-beta 1. Dev Biol. 1992; 152:354–362. [PubMed: 1644225]

Stabellini G, Locci P, Calvitti M, Evangelisti R, Marinucci L, Bodo M, Caruso A, Canaider S, Carinci P. Epithelial-mesenchymal interactions and lung branching morphogenesis. Role of polyamines and transforming growth factor beta1. Eur J Histochem. 2001; 45:151–162. [PubMed: 11512636]

Suki B. Fluctuations and power laws in pulmonary physiology. Am J Respir Crit Care Med. 2002; 166:133–137. [PubMed: 12119222]

Suki B, Barabasi AL, Hantos Z, Petak F, Stanley HE. Avalanches and power-law behaviour in lung inflation. Nature. 1994; 368:615–618. [PubMed: 8145846]

Tang N, Marshall WF, McMahon M, Metzger RJ, Martin GR. Control of mitotic spindle angle by the RAS-regulated ERK1/2 pathway determines lung tube shape. Science. 2011; 333:342–345. [PubMed: 21764747]

Trowell OA. The culture of mature organs in a synthetic medium. Exp Cell Res. 1959; 16:118–147. [PubMed: 13639945]

Warburton D, El-Hashash A, Carraro G, Tiozzo C, Sala F, Rogers O, Langhe SD, Kemp PJ, Riccardi D, Torday J, Bellusci S, Shi W, Lubkin SR, Jesudason E. Lung Organogenesis. Curr Top Dev Biol. 2010; 90C:73–158. [PubMed: 20691848]

Weaver M, Dunn NR, Hogan BL. Bmp4 and Fgf10 play opposing roles during lung bud morphogenesis. Development. 2000; 127:2695–2704. [PubMed: 10821767]

Weaver M, Yingling JM, Dunn NR, Bellusci S, Hogan BL. Bmp signaling regulates proximal-distal differentiation of endoderm in mouse lung development. Development. 1999; 126:4005–4015. [PubMed: 10457010]

Yu PB, Hong CC, Sachidanandan C, Babitt JL, Deng DY, Hoyng SA, Lin HY, Bloch KD, Peterson RT. Dorsomorphin inhibits BMP signals required for embryogenesis and iron metabolism. Nat Chem Biol. 2008; 4:33–41. [PubMed: 18026094]

Zhao J, Bu D, Lee M, Slavkin HC, Hall FL, Warburton D. Abrogation of transforming growth factor-beta type II receptor stimulates embryonic mouse lung branching morphogenesis in culture. Dev Biol. 1996; 180:242–257. [PubMed: 8948588]

Zhao J, Shi W, Chen H, Warburton D. Smad7 and Smad6 differentially modulate transforming growth factor beta -induced inhibition of embryonic lung morphogenesis. J Biol Chem. 2000; 275:23992–23997. [PubMed: 10801843]

Zhao J, Sime PJ, Bringas P Jr, Gauldie J, Warburton D. Epithelium-specific adenoviral transfer of a dominant-negative mutant TGF-beta type II receptor stimulates embryonic lung branching morphogenesis in culture and potentiates EGF and PDGF-AA. Mech Dev. 1998; 72:89–100. [PubMed: 9533955]

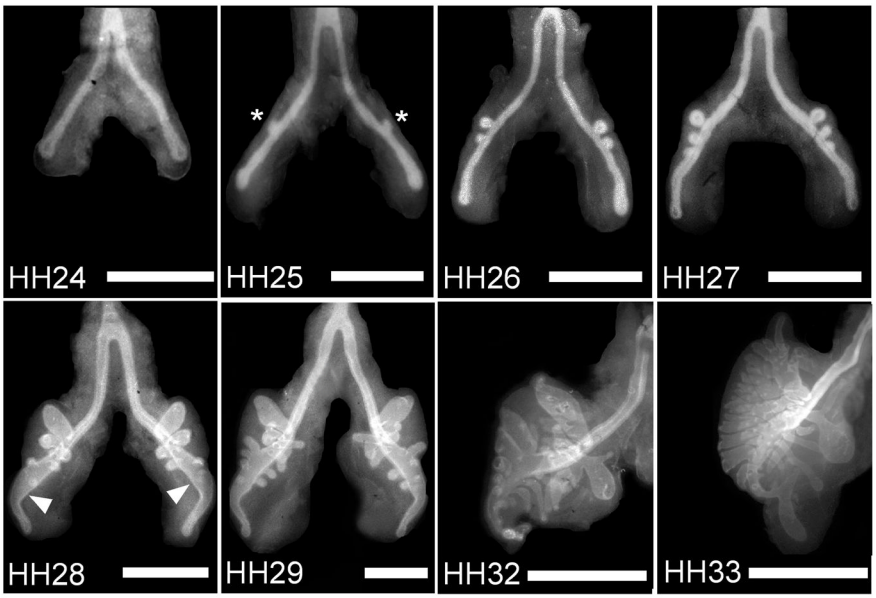

Figure 1.
Development of embryonic chicken airways over time. Immunofluorescence images of whole mount staining for E-cadherin in chicken lungs (developmental stages HH24-33) reveal a monopodial branching pattern. Asterisks denote examples of emerging secondary bronchi; arrowheads indicate the vestibulum. Scale bars, 500 μm.

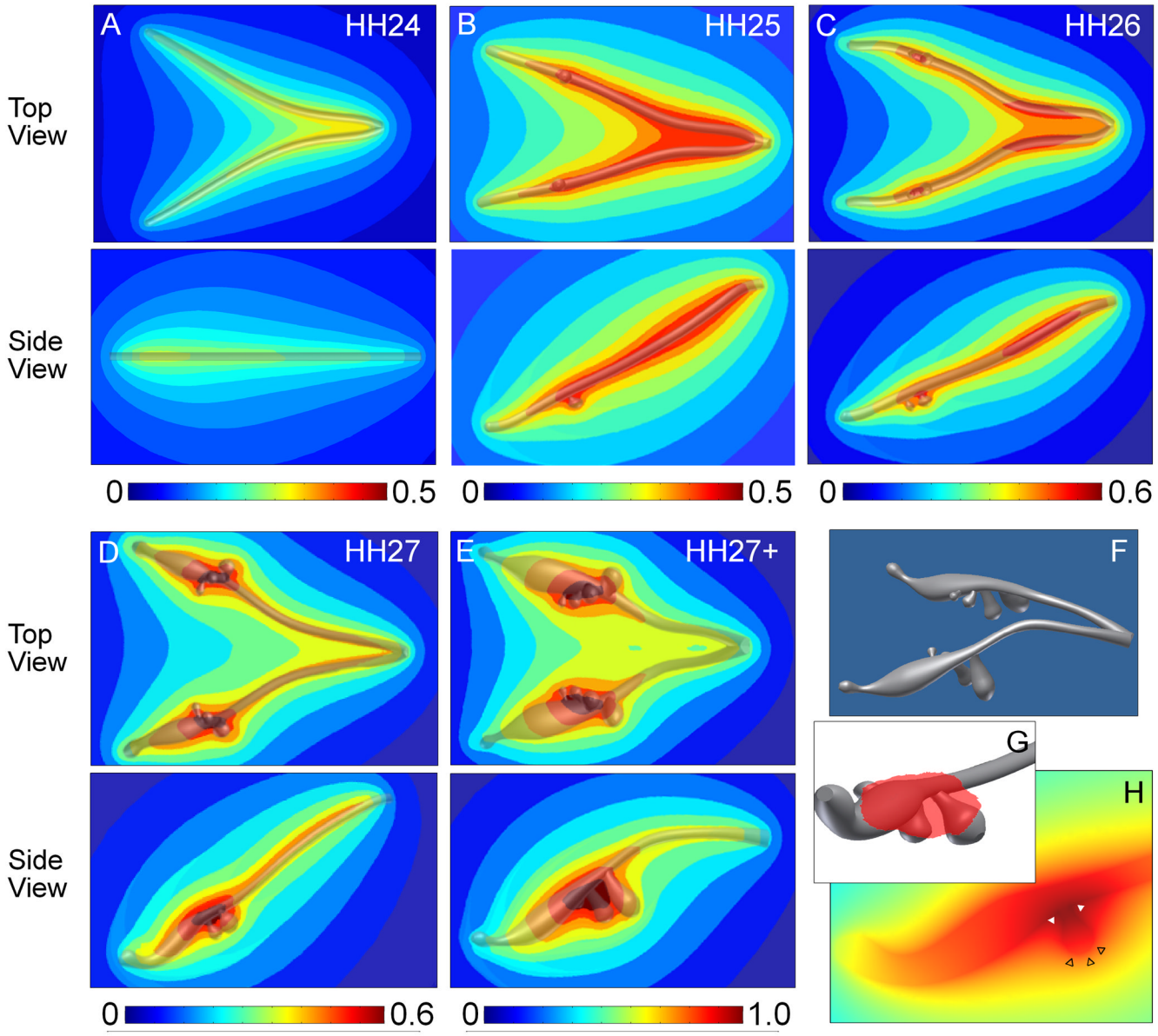

Figure 2.

Computational analysis of morphogen concentration and distribution in developing chicken lungs. (A–E) Predicted concentration profiles of a hypothetical morphogen uniformly secreted from the epithelium at various developmental stages. The concentration profiles are normalized to the highest value calculated for the HH27+ model, with red indicating areas of highest relative concentration and blue representing regions of low morphogen concentration. (F) An example solid model (HH27+) used for FEM analysis that was created from dimensions of E-cadherin-stained lung explants. (G) 3D solid model representation of the region of highest morphogen concentration represented by the red shading and (H) cross-section plot through a bud plotting morphogen concentration, which illustrates that the bud stalk and branch point have a local maximum (solid white triangles) whereas the bud tip has a local minimum (empty black triangles) in predicted morphogen concentration.

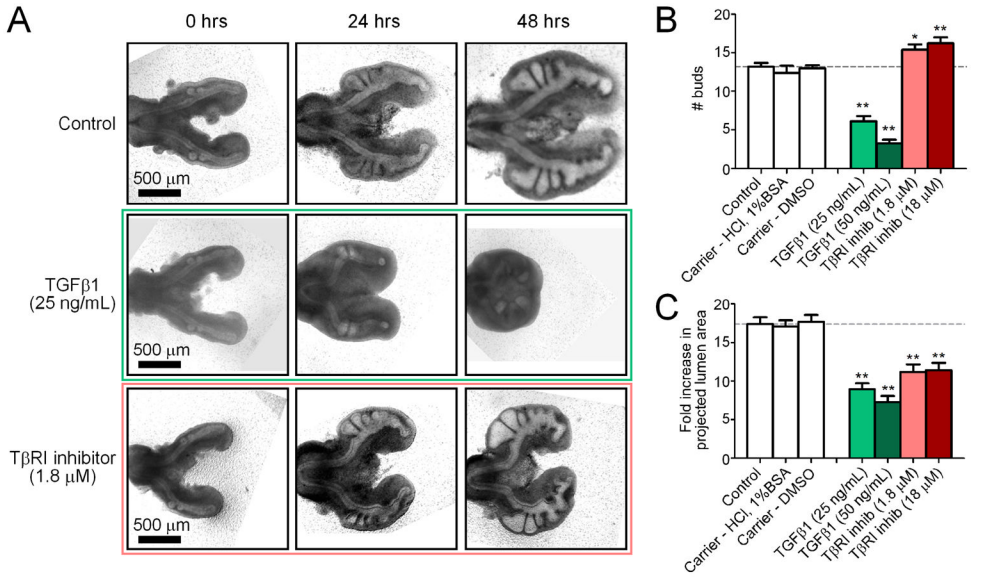

Figure 3.

Effect of disrupting the endogenous TGFβ concentration *ex vivo*. (A) Representative brightfield images of lungs cultured over 48 hours with recombinant TGFβ1, TβRI inhibitor, or control. Images are for the same explants tracked over time. Quantitative measures of bud enumeration (B) and fold increase in projected lumen area (C) of treated lungs after 48 hours of culture. Data +/− SEM (n>10), * p<0.05, ** p<0.001 relative to controls.

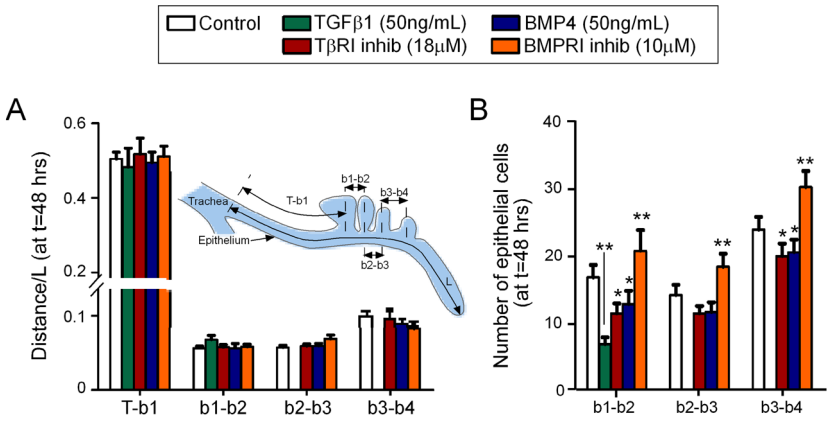

Figure 4.

Relative position of secondary bronchi along the primary bronchus. (A) Distance of each bud (*b1, b2, b3, b4*) normalized to the length of the primary bronchus (*L*), as measured from the tracheal bifurcation (*T*). (B) Average number of epithelial cells along the primary bronchus between subsequent secondary bronchi. Data +/− SEM (n>10), * p<0.05, ** p<0.001 relative to controls.

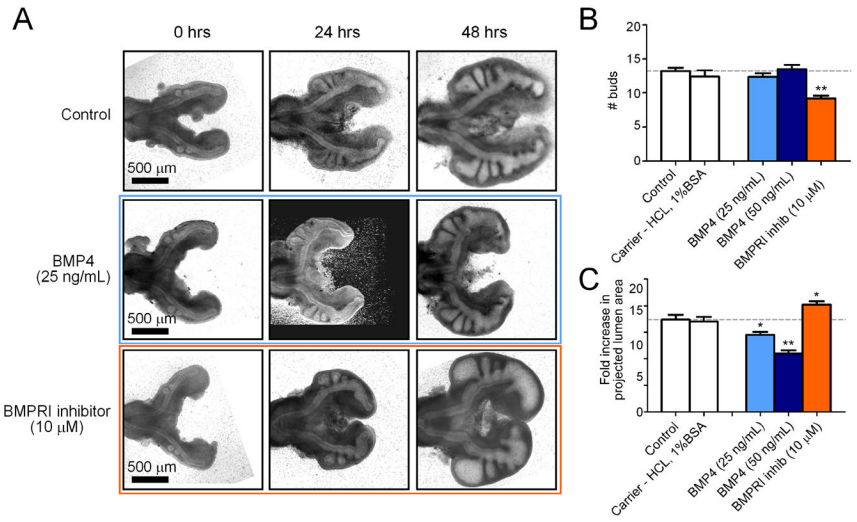

Figure 5.

Effect of disrupting the endogenous BMP concentration *ex vivo*. (A) Representative brightfield images of lungs cultured over 48 hours with recombinant BMP4, BMPRI inhibitor, or control. Images are for the same explants tracked over time. Quantitative measures of bud enumeration (B) and fold increase in projected lumen area (C) of treated lungs after 48 hours of culture. Data +/− SEM (n>10), * p<0.05, ** p<0.001 relative to controls.

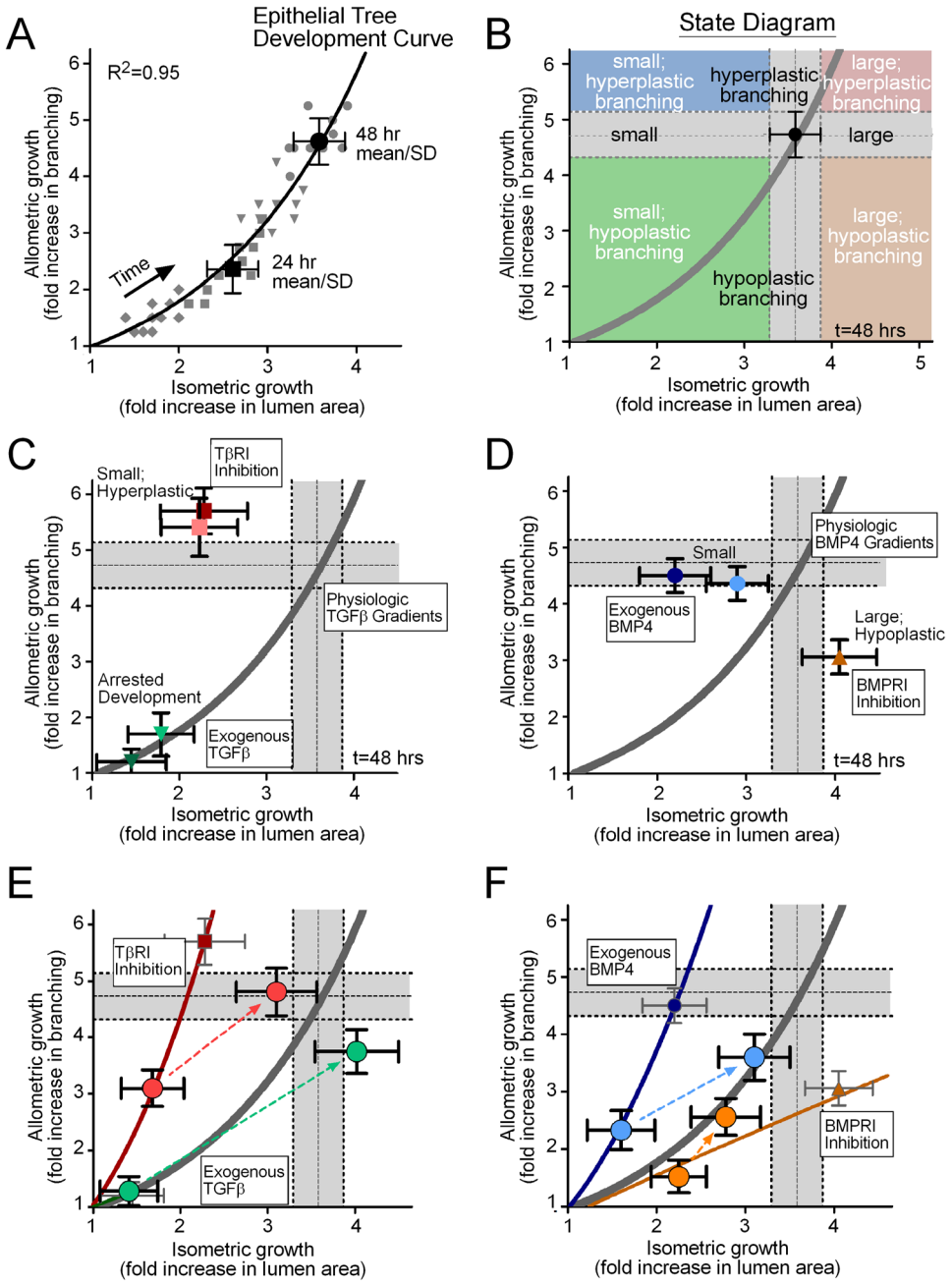

Figure 6.

Allometric analysis of lung explants. (A) Data from individual cultured lung explants at different time points (grey diamonds = 12hrs, squares = 24hrs, triangles = 36hrs, circles = 48hrs) collapse onto a single power-law curve that describes the relationship between allometric and isometric growth. The model curve (solid line) was fit to all of the individual data points (grey symbols) over all time intervals, and the 24 and 48 hour mean +/− SD are shown for reference. This model defines a master “development curve” for the epithelial tree. (B) An example “state diagram” that can be created for a given time of development, delineating parameter spaces that define small, equivalent, and large lungs, in addition to hypoplastic, equivalent, and hyperplastic branching. The grey bars indicate the 48 hour

mean +/− SD and are used as a visual reference to describe control explants. Allometry plots demonstrating the effects of (C) recombinant TGFβ1 (25ng/mL = light green, 50ng/mL = dark green) and TβRI inhibitor (1.8μM = light red, 18μM = dark red), and (D) recombinant BMP4 (25ng/mL = light blue, 50ng/mL = dark blue) and BMPRI inhibitor (10μM = orange). (E,F) Allometry plots detailing the resulting morphology from washout of the reagent after 24 hrs of culture. Thin solid lines are power-law models fit to the data from explants treated for 48 hours. Large circle data points represent 24 and 48 hour mean +/− SD for treatment groups and dotted lines represent the trajectory from 24 to 48 hours following treatment washout.

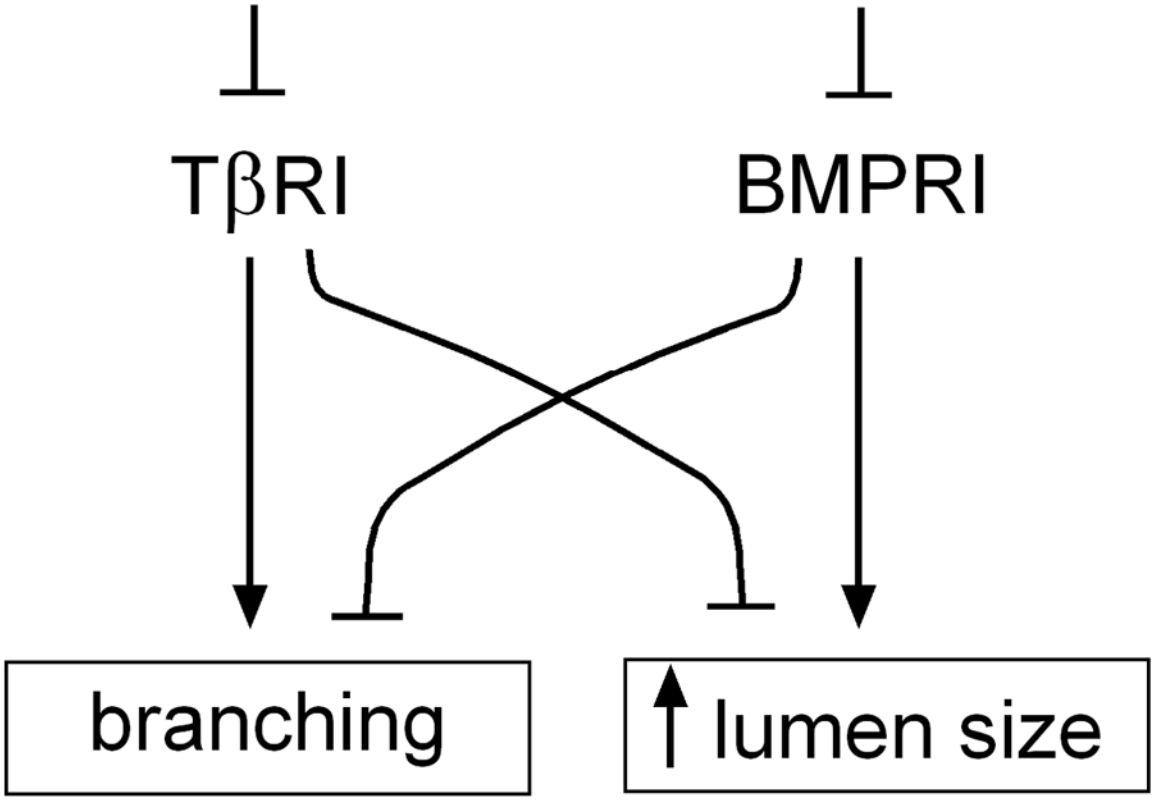

Figure 7.
Schematic diagram detailing the effects of TβRI and BMPRI inhibition on branching and lumen size in the chicken lung.